Available online at www.sciencedirect.com
SCIENCE DIRECT®

ELSEVIER

International Journal of Thermal Sciences 43 (2004) 95–104

International Journal of Thermal Sciences

www.elsevier.com/locate/ijts

Estimation of surface condition from the theory of dynamic thermal stresses

Han-Taw Chen *, Xin-Yi Wu, Yuan-San Hsiao

Department of Mechanical Engineering, National Cheng Kung University, Tainan 701, Taiwan, ROC

Received 24 June 2002; accepted 14 April 2003

Abstract

The present study applies a hybrid numerical algorithm of the Laplace transform technique and the finite-difference method with a sequential-in-time concept and the least-squares scheme to predict the unknown surface condition from the theory of dynamic thermal stresses. The unknown surface condition is not given a priori and is assumed to be the function of time before performing the inverse calculation. The whole time domain is divided into several analysis sub-time intervals and then the unknown surface condition on each analysis interval can be estimated from the transient displacement measurements or the transient temperature measurements. In order to show the efficiency and accuracy of the present inverse scheme, the comparison between the present estimates, the exact solution and the previous estimated results is demonstrated. The results show that a good estimation on the unknown surface condition can be obtained only at one selected location even for the case with the measurement error. The effect of the measurement location and the measurement error will also be investigated.

Keywords: Inverse problem; Surface condition; Hybrid method; Theory of dynamic thermal stresses

1. Introduction

It is usually assumed that the boundary conditions are accurately given in both theoretical and industrial applications. In many heat transfer situations, however, it is difficult to measure the approximate boundary conditions of a real problem such as combustion chambers, nuclear reactors, heat exchangers and re-entry vehicles, and so on. Thus such a problem has gradually become an interesting subject. In general, the inverse heat conduction problems (IHCP) were regarded as the estimation of the surface temperature and the heat flux from measured temperatures inside the conducting material. To date, many methods [1–5], such as the regularization, conjugate gradient and function specification methods, have been developed for the IHCP. Most of these works were only restricted to the IHCP using the temperature measurements. However, the thermocouple may not be the most appropriate sensor to obtain the internal measurements. This means that the additional information given by the moiré fringe photos or strain gages [6] can be tried to solve the IHCP. A few investigators [7,8] predicted the unknown surface condition from the viewpoint of the thermal stresses theory. Grysa et al. [7] applied the thermal stresses theory in conjunction with the Laplace transform method to investigate the inverse problem of the temperature field from the temperature, heat flux and displacement measurements inside the solid. It can be observed from their work that the inversion of the unknown surface temperature in the transform domain was complicated. Thus it is difficult to invert the unknown surface temperature in the transform domain to the physical quantity. In order to obtain a more accurate estimated result, the measurement location can necessarily be located near the position of the unknown boundary condition. In addition, their estimated results were also sensitive to the internal measurements and the magnitude of the time step. Blanc and Raynaud [8] applied a simple analysis in conjunction with the quasi-static and uncoupled assumptions to estimate the unknown boundary condition of an inverse problem using the thermal strain and temperature measurements instead of the temperature measurements only.

The literature reviews showed that Sparrow et al. [9], Woo and Chow [10], Monde [11], Chen and Chang [12], Chen et al. [13–15] and Chen and Wu [16] applied the

* Corresponding author.
E-mail address: htchen@mail.ncku.edu.tw (H.-T. Chen).

1290-0729/$ – see front matter
doi:10.1016/S1290-0729(03)00105-4

Nomenclature

C_j	undetermined coefficient	
c_0	parameter, $= \sqrt{2G(1-\nu)/[\rho(1-2\nu)]}$	
d_j	small value defined in Eq. (32)	
d_j^*	correction of C_j defined in Eq. (38)	
$F_1(t)$	unknown surface temperature	
$\{F_T\}$	forcing matrix for the temperature field	
$\{F_u\}$	forcing matrix for the displacement field	
G	shear modulus	
I	symbol for temperature or displacement	
k_0	parameter, $= (1+\nu)\alpha_t/(1-\nu)$	
$\{K_T\}$	global matrix for the temperature field	
$\{K_u\}$	global matrix for the displacement field	
L	thickness of the tested slab	m
ℓ	distance between two neighboring nodes	m
M	number of sub-time domains	
M_t	number of the discrete measurement times	
N	degree of a polynomial guess function	
n	total number of nodes	
q	unknown surface heat flux	$\mathrm{W{\cdot}m^{-2}}$
s	Laplace transform parameter	
T	temperature	°C
$\widetilde{T}$	temperature in the transform domain defined in Eq. (16)	
$\{\widetilde{T}\}$	global matrix of the nodal temperatures in the transform domain	
t	time	s
t_f	final time	s
t_0	initial measurement time	s
t_r	discrete measurement time	s
t^*	dimensionless time, $= \alpha t/L^2$	
Δt_e	measurement time step	s
Δt_e^*	dimensionless measurement time step, $= \alpha\Delta t_e/L^2$	
Δt_s^*	dimensionless time step, $= \alpha\Delta t_e/\ell^2$	
u	displacement	m
$\tilde{u}$	displacement in the transform domain defined in Eq. (17)	
$\{\tilde{u}\}$	global matrix of the nodal displacements in the transform domain	
$\tilde{u}_1$	displacement in the transform domain at $x = 0$	
x	spatial coordinate	m
x_m	measurement location	m

Greek symbols

α	thermal diffusivity	$\mathrm{m^2{\cdot}s^{-1}}$
α_t	coefficient of linear thermal expansion	
ε	prescribed accuracy	
ξ	dimensionless spatial coordinate, $= x/L$	
ν	Poisson ratio	
ρ	density	$\mathrm{kg{\cdot}m^{-3}}$
σ	normal stress	$\mathrm{N{\cdot}m^{-2}}$
σ_{cur}	standard deviation with respect to curve-fitted results	
σ_{exa}	standard deviation with respect to exact data	
ω	averaged random error	

Subscripts

cal	calculated value
cur	curve-fitted value
exa	exact solution
mea	measured data

Laplace transform method to predict the unknown surface condition from the temperature measurements only. Most numerical schemes for the IHCP may be sensitive to measurement noises. It is known that this sensitivity depends on the time step. In general, the smaller the time step, the more ill-posed the problem. In order to improve this drawback, Chen and Chang [12] introduced a hybrid scheme of the Laplace transform and finite-difference methods to estimate the unknown surface temperature in one-dimensional IHCP using the measured temperatures inside the material without measurement errors. Similarly, the measurement location had better be located near the position of the unknown boundary condition in order to obtain a more accurate estimated result. Due to this drawback, Chen et al. [13–15] and Chen and Wu [16] applied the similar scheme in conjunction with a sequential-in-time concept and the least-squares method to estimate the unknown surface condition from the temperature measurements. It can be observed from the works of Chen et al. [13–15] and Chen and Wu [16] that the estimates of the unknown surface condition are in good agreement with the exact solution of the direct problem provided the measurement error is not considered. In addition, the estimated results of these previous works [13–16] also displayed that the effects of the measurement time step and the measurement error on the estimates were not very significant. It can be found from the work of Chen and Wu [16] that the estimation of the unknown surface temperature obtained from the present inverse scheme is also in good agreement with experimental temperature data [17]. Li [17] applied the implicit finite-difference method in conjunction with the linear least-squares errors method to predict the unknown surface temperature with the Dirichlet boundary conditions. It can be observed that Li's predicated results [14] did not agree well with his experimental temperature data for short times.

The present study applies the similar hybrid method [13–16] to estimate the unknown boundary condition from the theory of dynamic thermal stresses using the displacement and temperature measurements. Due to the application of the Laplace transform, the stability limit $\alpha\Delta t/\ell^2$ does not appear in the present inverse scheme. In order to show the efficiency and accuracy of the present inverse scheme,

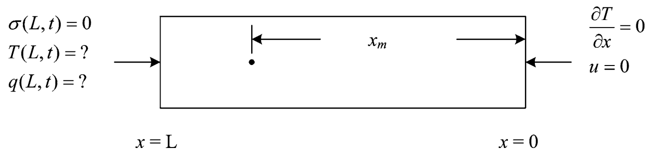

Fig. 1. Schematic diagram of the inverse problem.

problems with various types of the boundary conditions will be illustrated. Methods using the temperature and displacement measurements are respectively denoted as the T- and u-methods.

2. Mathematical formulation

The mathematical formulation and the basic assumptions established in the present study come from the work of Grysa et al. [7]. The IHCP investigated here involves the estimation of the unknown surface condition at the surface $x = L$ from the transient displacement and temperature measurements inside the body. The present study is limited to the unidirectional problem, as shown in Fig. 1. A slab with the finite thickness L, initially at a uniform temperature, is insulated at the surface $x = 0$, while the surface at $x = L$ is heated uniformly. For the direct problem, the temperature and displacement fields can be determined provided that the surface conditions at $x = 0$ and $x = L$ are given. However, one of the surface conditions is unknown for the inverse problem. This unknown surface condition can be estimated provided that the additional information of the transient temperature measurements or the transient displacement measurements can be obtained. In order to demonstrate the flexibility of the present inverse scheme, various types of the boundary conditions will be illustrated in the present study.

The relationship of the stress $\sigma(x,t)$, the displacement $u(x,t)$ and the temperature $T(x,t)$ can be obtained from the one-dimensional Duhamel–Neumann equation with constant material properties in terms of the shear modulus G [7, 18].

$$\sigma(x,t) = \frac{2G}{1-2\nu}\left[(1-\nu)\frac{\partial u(x,t)}{\partial x} - (1+\nu)\alpha_t T(x,t)\right] \quad (1)$$

where t is time, x is the spatial coordinate, ν is the Poisson ratio and α_t is the coefficient of linear thermal expansion.

It is assumed that the motion of particles of the body is slow. Thus the conservation principle of linear momentum in the absence of the body force may be written in the form [18]

$$\frac{\partial \sigma(x,t)}{\partial x} = \rho\frac{\partial^2 u(x,t)}{\partial t^2} \quad (2)$$

where ρ is the density.

The substitution of Eq. (1) into Eq. (2) yields the equation of motion in the displacement as

$$\frac{\partial^2 u}{\partial x^2} - \frac{1}{c_0^2}\frac{\partial^2 u}{\partial t^2} = k_0\frac{\partial T}{\partial x} \quad \text{in } 0 < x < L,\ 0 < t \leqslant t_f \quad (3)$$

where the parameters k_0 and c_0 are defined as $k_0 = ((1+\nu)/(1-\nu))\alpha_t$ and $c_0 = \sqrt{2G(1-\nu)/[\rho(1-2\nu)]}$. t_f is the final time.

The one-dimensional heat conduction equation with constant thermal properties can be expressed as

$$\frac{\partial^2 T}{\partial x^2} = \frac{1}{\alpha}\frac{\partial T}{\partial t} \quad \text{in } 0 < x < L,\ 0 < t \leqslant t_f \quad (4)$$

where α is the thermal diffusivity.

The present inverse problem is subject to the following boundary conditions and the initial conditions.

$$\frac{\partial T(0,t)}{\partial x} = 0 \quad \text{and} \quad T(L,t) = F_1(t) \quad (5)$$

$$u(0,t) = 0 \quad \text{and} \quad \sigma(L,t) = 0 \quad (6)$$

and

$$T(x,0) = 0, \quad u(x,0) = 0 \quad \text{and} \quad \frac{\partial u(x,0)}{\partial t} = 0 \quad (7)$$

Assume that $F_1(t)$ in Eq. (5) is unknown. It can be estimated provided that the interior temperature measurements or the interior displacement measurement in the slab can be given.

3. Numerical analysis

In order to obtain the additional information, the measured temperature history or the measured displacement history at a certain location of the tested material can be obtained by using the thermocouple or the moiré fringe photos [6]. These temperature and displacement measurements are, respectively, denoted by $T_{\text{mea}}(x_m,t_r)$ and $u_{\text{mea}}(x_m,t_r)$, $r = 0,\ldots,M_t-1$, where x_m is the measurement location, t_r is the discrete measurement time and M_t denotes the number of the discrete measurement times. It worth mentioning that these interior measurements can be taken from an initial measurement time $t_0 (t_r \geqslant t_0)$ for the present inverse scheme.

In real industrial applications, the experimental measured values often exhibit random oscillations due to experimental uncertainty [16,17]. Thus, in order to simulate the experimental measured data, $T_{\text{mea}}(x_m,t_r)$ and $u_{\text{mea}}(x_m,t_r)$ can be modified by adding small random errors to the exact solution of the direct problem. On the other hand, $T_{\text{mea}}(x_m,t_r)$ and $u_{\text{mea}}(x_m,t_r)$ used in the present inverse analysis can be expressed as

$$I_{\text{mea}}(x_m,t_r) = I_{\text{exa}}(x_m,t_r)(1+\omega) \quad \text{for } r = 0,\ldots,M_t-1 \quad (8)$$

where I denotes the temperature T or the displacement u. ω represents the averaged random error.

An approximate polynomial function in conjunction with the least-squares method can be used to fit the experimental measured data [19]. The curve-fitted values are obtained from this polynomial function.

The standard deviations of the temperature and displacement measurements with respect to the exact solution and the curve-fitted values of the experimental measured data are respectively defined as [19]

$$\sigma_{\text{exa}} = \frac{1}{M_t}\left[\sum_{r=0}^{M_t-1}\big(I_{\text{mea}}(x_m,t_r) - I_{\text{exa}}(x_m,t_r)\big)^2\right]^{1/2} \tag{9}$$

and

$$\sigma_{\text{cur}} = \frac{1}{M_t}\left[\sum_{r=0}^{M_t-1}\big(I_{\text{mea}}(x_m,t_r) - I_{\text{cur}}(x_m,t_r)\big)^2\right]^{1/2} \tag{10}$$

The method of the Laplace transform is applied to remove the time-dependent terms from the governing differential equations and the boundary conditions. Thus, the Laplace transforms of Eqs. (3)–(6) with respect to t in conjunction with Eqs. (1) and (7) are

$$\frac{\mathrm{d}^2\tilde{u}}{\mathrm{d}x^2} - \frac{s^2}{c_0^2}\tilde{u} = k_0\frac{\mathrm{d}\widetilde{T}}{\mathrm{d}x} \quad \text{for } 0 < x < L \tag{11}$$

$$\frac{\mathrm{d}^2\widetilde{T}}{\mathrm{d}x^2} - \frac{s}{\alpha}\widetilde{T} = 0 \quad \text{for } 0 < x < L \tag{12}$$

with

$$\frac{\mathrm{d}\widetilde{T}(0,s)}{\mathrm{d}x} = 0 \quad \text{and} \quad \widetilde{T}(L,s) = \widetilde{F}_1(s) \tag{13}$$

and

$$\tilde{u}(0,s) = 0 \tag{14}$$

$$(1-\nu)\frac{\mathrm{d}\tilde{u}}{\mathrm{d}x}(L,s) - (1+\nu)\alpha_t\widetilde{T}(L,s) = 0 \tag{15}$$

where s is the Laplace transform parameter. $\widetilde{T}$ and $\tilde{u}$ are defined as

$$\widetilde{T}(x,s) = \int_0^\infty T(x,t)\,\mathrm{e}^{-st}\,\mathrm{d}t \tag{16}$$

and

$$\tilde{u}(x,s) = \int_0^\infty u(x,t)\,\mathrm{e}^{-st}\,\mathrm{d}t \tag{17}$$

The finite-difference forms of Eqs. (11)–(15) are given as

$$\frac{\tilde{u}_{i+1} - 2\tilde{u}_i + \tilde{u}_{i-1}}{\ell^2} - \frac{s^2}{c_0^2}\tilde{u}_i = k_0\frac{\widetilde{T}_{i+1} - \widetilde{T}_{i-1}}{2\ell} \quad \text{for } 1 \leqslant i \leqslant n \tag{18}$$

$$\frac{\widetilde{T}_{i+1} - 2\widetilde{T}_i + \widetilde{T}_{i-1}}{\ell^2} - \frac{s}{\alpha}\widetilde{T}_i = 0 \quad \text{for } 1 \leqslant i \leqslant n \tag{19}$$

$$\widetilde{T}_2 = \widetilde{T}_0 \tag{20}$$

$$\widetilde{T}(L,s) = \widetilde{T}_n = \widetilde{F}_1(s) \tag{21}$$

$$\tilde{u}(0,s) = \tilde{u}_1 = 0 \tag{22}$$

and

$$(1-\nu)(\tilde{u}_{n+1} - \tilde{u}_{n-1}) - 2\ell(1+\nu)\alpha_t\widetilde{T}_n = 0 \tag{23}$$

where $\ell = L/(n-1)$ denotes the distance between two neighboring nodes and is uniform. n is the total number of nodes.

Elimination of $\widetilde{T}_0$ between Eq. (19) for $i = 1$ and Eq. (20) gives

$$-\left(\frac{1}{\ell^2} + \frac{s}{2\alpha}\right)\widetilde{T}_1 + \frac{\widetilde{T}_2}{\ell^2} = 0 \tag{24}$$

where $\widetilde{T}_1$ denotes the temperature in the transform domain at $x = 0$.

Eliminating the $\widetilde{T}_{n+1}$ term of Eqs. (18) and (19) for $i = n$ and then canceling the $\tilde{u}_{n+1}$ term of the resulting form and Eq. (23) can give

$$2\frac{\tilde{u}_{n-1}}{\ell^2} - \left(\frac{2}{\ell^2} + \frac{s^2}{c_0^2}\right)\tilde{u}_n = -\frac{k_0\widetilde{T}_{n-1}}{2\ell} + \left[\frac{s\ell k_0}{2\alpha} + \frac{k_0}{\ell} - \frac{2(1+\nu)\alpha_t}{(1-\nu)\ell}\right]\widetilde{T}_n \tag{25}$$

The arrangement of Eqs. (19), (21) and (24) can yield the matrix equation for the nodal temperatures as

$$[K_T]\{\widetilde{T}\} = \{F_T\} \tag{26}$$

The arrangement of Eqs. (18), (22) and (25) yields the matrix equation for the nodal displacements as

$$[K_u]\{\tilde{u}\} = \{F_u\} \tag{27}$$

where $[K_T]$ and $[K_u]$ are the matrices with the Laplace parameter s for the temperature and displacement fields, respectively. $\{\widetilde{T}\}$ and $\{\tilde{u}\}$ are the matrices representing the unknown nodal temperatures and displacements in the transform domain. $\{F_T\}$ and $\{F_u\}$, respectively, are the matrices representing the forcing terms for the temperature and displacement fields. It should be noted that the forcing term $\{F_u\}$ involves the transformed nodal temperature. *Owing to the uncoupled assumption in the present study, the direct Gauss elimination method can be first applied to determine the transformed nodal temperatures from Eq.* (26). *Afterwards, in accordance with these obtained transformed nodal temperatures, the transformed nodal displacements can be obtained from Eq.* (27). *The resulting transformed nodal temperatures and nodal displacements can be inverted to the physical quantities using the numerical inversion of the Laplace transform* [20–22]. *For the T-method, only Eq.* (26) *is applied to perform the inverse calculation. However, both Eqs.* (26) *and* (27) *must be solved for the u-method.*

The unknown surface temperature $F_1(t)$ is assumed to be the function of time before performing the inverse calculation. However, it is not easy to obtain an approximate polynomial function that can completely fit this unknown function $F_1(t)$ over the whole time domain considered. Under this circumstance, a sequential-in-time procedure can be introduced to estimate $F_1(t)$. On the other hand, the whole time domain $t_0 \leqslant t \leqslant t_f$ will be divided into M sub-time domains. The discrete measurement time t_r can be defined as $t_r = t_0 + r\Delta t_e$ $(r = 0, 1, \ldots, M_t - 1)$, where the measurement time step Δt_e is defined as $\Delta t_e = (t_f - t_0)/(M_t - 1)$. Due to the application of the Laplace transform in the present study, t_0 is not always the initial time $t = 0$. The unknown surface temperature $F_1(t)$ on each analysis interval can be approximated by the $(N-1)$th degree polynomial guess function of time and is expressed as

$$F_1(t) = \sum_{j=1}^{N} C_j t^{j-1} \tag{28}$$

where C_j $(j = 1, 2, \ldots, N)$ is the unknown coefficient and is estimated using the least-squares method in conjunction with the measured data on each analysis interval. Based on the definitions of N, M and M_t, the M_t value is equal to "$MN - M + 1$".

The least-squares minimization technique is applied to minimize the sum of the squares of the deviations between the calculated values and the curve-fitted results at the measurement location x_m. The error in the estimate $E(C_1, C_2, \ldots, C_N)$ on each analysis interval $t_i \leqslant t_r \leqslant t_{i+N-1}$ $(i = 0, N-1, 2(N-1), \ldots, M_t - N)$ can be expressed as

$$E(C_1, C_2, \ldots, C_N) = \sum_{r=i}^{i+N-1} \left[I_{\mathrm{cal}}(x_m, t_r) - I_{\mathrm{cur}}(x_m, t_r)\right]^2 \tag{29}$$

where $I_{\mathrm{cal}}(x_m, t_r)$ denotes the calculated temperature or the calculated displacement. $I_{\mathrm{cur}}(x_m, t_r)$ is obtained from the curve-fitted profile of the experimental measured data. The estimated values of C_j $(j = 1, 2, \ldots, N)$ are determined provided that the value of $E(C_1, C_2, \ldots, C_N)$ is minimum. The computational procedures for estimating the unknown coefficient C_j $(j = 1, 2, \ldots, N)$ are described as follows.

First, the initial guesses of C_j $(j = 1, 2, \ldots, N)$ are given. Afterwards, the calculated temperatures and displacements at $x = x_m$ are, respectively, determined from Eqs. (26) and (27). Deviations of $I_{\mathrm{cur}}(x_m, t_r)$ and $I_{\mathrm{cal}}(x_m, t_r)$ on each analysis interval $t_i \leqslant t_r \leqslant t_{i+N-1}$ $(i = 0, N-1, 2(N-1), \ldots, M_t - N)$ are expressed as

$$e_p = I_{\mathrm{cal}}(x_m, t_r) - I_{\mathrm{cur}}(x_m, t_r) \quad \text{for } p = r - i + 1,\ i \leqslant r \leqslant i + N - 1 \tag{30}$$

The new calculated value $I^p_{\mathrm{cal}}(x_m, t_r)$ on each analysis interval $t_i \leqslant t_r \leqslant t_{i+N-1}$ $(i = 0, N-1, 2(N-1), \ldots, M_t - N)$ can be expanded in a first-order Taylor series as

$$I^p_{\mathrm{cal}}(x_m, t_r) = I_{\mathrm{cal}}(x_m, t_r) + \sum_{j=1}^{N} \frac{\partial I_{\mathrm{cal}}}{\partial C_j}\, dC_j \quad \text{for } p = r - i + 1,\ i \leqslant r \leqslant i + N - 1 \tag{31}$$

In order to obtain the derivative $\partial I_{\mathrm{cal}}/\partial C_j$ in Eq. (31), the new unknown coefficient C^*_j is introduced as

$$C^*_j = C_j + d_j \delta_{jk} \quad \text{for } j, k = 1, 2, \ldots, N \tag{32}$$

where $d_j = C^*_j - C_j$ is a small value corresponding to C_j. The symbol δ_{jk} is Kronecker delta.

Similarly, the new calculated value $I^p_{\mathrm{cal}}(x_m, t_r)$ with respect to C^*_j shown in Eq. (32) can also be determined from Eq. (26) or Eq. (27). Deviations between $I^p_{\mathrm{cal}}(x_m, t_r)$ and $I_{\mathrm{cur}}(x_m, t_r)$ on each analysis interval $t_i \leqslant t_r \leqslant t_{i+N-1}$ $(i = 0, N-1, 2(N-1), \ldots, M_t - N)$ can be written as

$$e^j_p = I^p_{\mathrm{cal}}(x_m, t_r) - I_{\mathrm{cur}}(x_m, t_r) \quad \text{for } j, p = 1, 2, \ldots, N \tag{33}$$

The finite-difference representation of the derivative $\partial I_{\mathrm{cal}}/\partial C_j$ can be expressed as

$$\omega^j_p = \frac{\partial I_{\mathrm{cal}}}{\partial C_j} = \frac{I^p_{\mathrm{cal}} - I_{\mathrm{cal}}}{C^*_j - C_j} \quad \text{for } j, p = 1, 2, \ldots, N \tag{34}$$

The substitution of Eqs. (30), (32) and (33) into Eq. (34) yields

$$\omega^j_p = \frac{e^j_p - e_p}{d_j} \tag{35}$$

Substituting Eq. (34) into Eq. (31) yields

$$I^p_{\mathrm{cal}}(x_m, t_r) = I_{\mathrm{cal}}(x_m, t_r) + \sum_{j=1}^{N} \omega^j_p d^*_j \quad \text{for } p = r - i + 1,\ i \leqslant r \leqslant i + N - 1 \tag{36}$$

where $d^*_j = \mathrm{d}C_j$ denotes the new correction of C_j.

Substituting Eqs. (30) and (33) into Eq. (36) yields

$$e^j_p = e_p + \sum_{j=1}^{N} \omega^j_p d^*_j \quad \text{for } p = 1, 2, \ldots, N \tag{37}$$

In accordance with Eqs. (29) and (33), the error in the estimate $E(C_1 + \Delta C_1, C_2 + \Delta C_2, \ldots, C_N + \Delta C_N)$ can be expressed as

$$E = \sum_{p=1}^{N} \left(e^j_p\right)^2 \tag{38}$$

In order to yield the minimum value of E with respect to C_j, differentiating E corresponding to the new corrections d^*_j is performed. Thus the correction equations corresponding to C_j can be expressed as

$$\sum_{j=1}^{N} \sum_{p=1}^{N} \omega^k_p \omega^j_p d^*_j = -\sum_{p=1}^{N} \omega^k_p e_p \quad \text{for } k = 1, 2, \ldots, N \tag{39}$$

Eq. (39) is a set of N algebraic equations for the new corrections. The new corrections d^*_j are obtained from this equation. Thereafter, the new coefficients of C_j, $C_j + d^*_j$, can be determined. The above numerical procedures are repeated until the value of $|(I_{\mathrm{cal}}(x_m, t_r) - I_{\mathrm{cur}}(x_m, t_r))/I_{\mathrm{cur}}(x_m, t_r)|$ is all less than a prescribed accuracy ε. In the present study, $\varepsilon = 0.001$ is taken through all the examples.

4. Numerical examples

In order to demonstrate the accuracy and efficiency of the present inverse scheme in estimating the unknown surface condition from the knowledge of the temperature measurements or the displacement measurements at any selected location of the tested material, various examples will be illustrated. These temperature measurements or the displacement measurements can be obtained by using the thermocouple or the moiré fringe photos [6] from an initial measurement time t_0. In all the test cases considered here, the $(N-1)$th degree polynomial guess function is selected to approximate the unknown function $F_1(t)$ on each sub-time domain. The numerical data used in the present study come from the work of Grysa et al. [7]. The following data are taken for calculations: $k_0 = 1.19 \times 10^{-8}\ \mathrm{m^2{\cdot}s^{-1}}$, $\alpha = 1.19 \times 10^{-5}\ \mathrm{m^2{\cdot}s^{-1}}$, $G = 7.9461 \times 10^{10}\ \mathrm{N{\cdot}m^{-2}}$, $L = 0.01$ m, $\nu = 0.3$, $\rho = 7.8 \times 10^3\ \mathrm{kg{\cdot}m^{-3}}$ and $\alpha_t = 12 \times 10^{-6}\ \mathrm{deg^{-1}}$. In the present study, the effect of the dimensionless measurement time step, space size, initial guesses and measurement error on the estimation of the unknown surface condition is also examined. All the computations are performed with the uniform space size ℓ.

4.1. Example 1 (Unknown surface temperature at $x = L$)

It is assumed that the unknown surface temperature at $x = L$, $F_1(t)$, will be estimated in this example. In order to estimate this unknown surface temperature $F_1(t)$, the additional information on the temperature measurements or the displacement measurements must be given. The fourth degree polynomial guess function ($N = 5$) is selected to approximate $F_1(t)$ on each sub-time domain for this inverse calculation.

The Laplace transform of Eq. (28) for $N = 5$ can yield $\widetilde{F}_1(t)$ as

$$\widetilde{F}_1(s) = \sum_{j=1}^{5} C_j \frac{\Gamma(j)}{s^j} \tag{40}$$

where $\Gamma(j)$ is the Gamma function.

The unknown coefficient C_j $(j = 1, 2, \ldots, 5)$, used to begin the iteration is taken as unity. $t_0 = 0$ s and $t_f = 30$ s are taken for the inverse calculation of this example. The temperature measurements or the displacement measurements are recorded every Δt_e value. For the convenience of the inverse calculation, the dimensionless time t^*, the dimensionless measurement time step Δt_e^*, the dimensionless time step Δt_s^*, the dimensionless spatial coordinate ξ and the dimensionless measurement location ξ_m are introduced. They are defined as $t^* = \alpha t/L^2$, $\Delta t_e^* = \alpha \Delta t_e/L^2$, $\Delta t_s^* = \alpha \Delta t_e/\ell^2$, $\xi = x/L$ and $\xi_m = x_m/L$. In order to evidence the accuracy of the present inverse scheme, the inverse problem with the unknown surface temperature $F_1(t) = 1$ proposed by Grysa et al. [7] is first illustrated. It is not very difficult to solve this inverse heat conduction problem. Thus the comparisons of the unknown surface temperature $F_1(t)$ and $T(L/2, t)$ among the present estimates, the estimates of Grysa et al. [7] and the exact solution for $\omega = 0$ and various Δt_e values at various measurement locations are, respectively, shown in Table 1 and Fig. 2. Table 1 shows the comparison among the present estimates, the estimates of Grysa et al. [7] and the exact solution $T_{\mathrm{exa}}(L/2, t)$ for $n = 11$, $\omega = 0$, $M = 6$ and $\Delta t_e = 1$ s ($\Delta t_s^* = 11.9$). It can be found from Table 1 that the estimates of Grysa et al. [7] for the early time ($t \leqslant 1$ s) can be poor even though the measurement location is close to the position of the estimated value. The difference between the estimates of Grysa et al. [7] and the exact solution $T_{\mathrm{exa}}(L/2, 1)$ goes up to 13.4%. However, the present estimates using the T- and u-methods agree well with the exact solution over the whole time domain considered for $\omega = 0$ even though the measurement location is located far from the position of the estimated value. For most of the previous works, the measurement location is generally located at the position close to the estimated value in order to obtain a more accurate estimate. The above results show that the present inverse scheme has good accuracy and good efficiency for the present inverse problem.

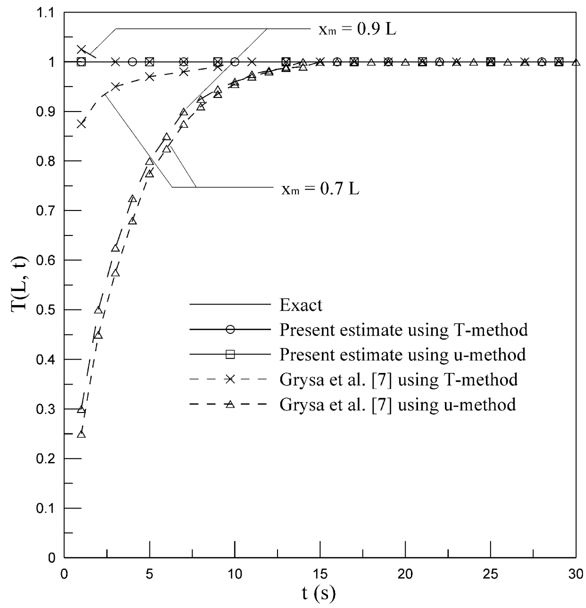

Fig. 2. Comparison of $T(L, t)$ for $F_1(t) = 1$, $\omega = 0$, $M = 3$, $\Delta t_e = 2$ s and $x_m = 0$.

In order to evidence the effect of the measurement time step Δt_e or the dimensionless time step Δt_s^* on the present estimates for $n = 11$, $\omega = 0$ and $M = 6$. We find that the present estimates using $\Delta t_e = 0.5$ s ($\Delta t_s^* = 5.95$) are in good agreement with those using $\Delta t_e = 1$ s ($\Delta t_s^* = 11.9$) and the exact solution $T_{\mathrm{exa}}(L/2, t)$ shown in Table 1. Thus, these present estimates are not shown in this paper.

The comparison among the present estimates for $n = 11$, $x_m = 0$, $\omega = 0$, $M = 3$ and $\Delta t_e = 2$ s ($\Delta t_s^* = 23.8$), the estimates of Grysa et al. [7] and the exact solution $T_{\mathrm{exa}}(L, t)$ is shown in Fig. 2 using the T- and u-methods. The effect of the measurement location on the unknown

Table 1
Comparison of $T(L/2,t)$ between the present estimates, the estimates of Grysa et al. [7] and the exact solution for $\omega = 0$, $M = 6$ and $\Delta t_e = 1$ s

t	Grysa et al. [7]	Present estimates		$T_{exa}(L/2,t)$
	T-method $x_m = 0.4L$	T-method $x_m = 0$	u-method $x_m = 0.1L$	
1	0.2663	0.3075	0.3075	0.3075
2	0.4734	0.4980	0.4980	0.4980
3	0.6090	0.6268	0.6268	0.6268
4	0.7068	0.7218	0.7218	0.7218
5	0.7828	0.7926	0.7926	0.7926
10	0.9499	0.9522	0.9522	0.9522
15	0.9885	0.9890	0.9890	0.9890
20	0.9973	0.9975	0.9975	0.9975

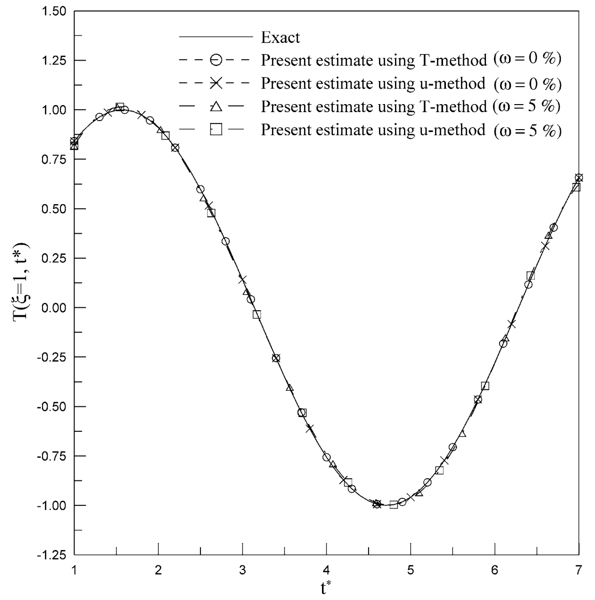

Fig. 3. Comparison of $T(\xi = 1, t^*)$ for $F_1(t^*) = \sin(t^*)$, $\xi_m = 0.1$ and various ω values.

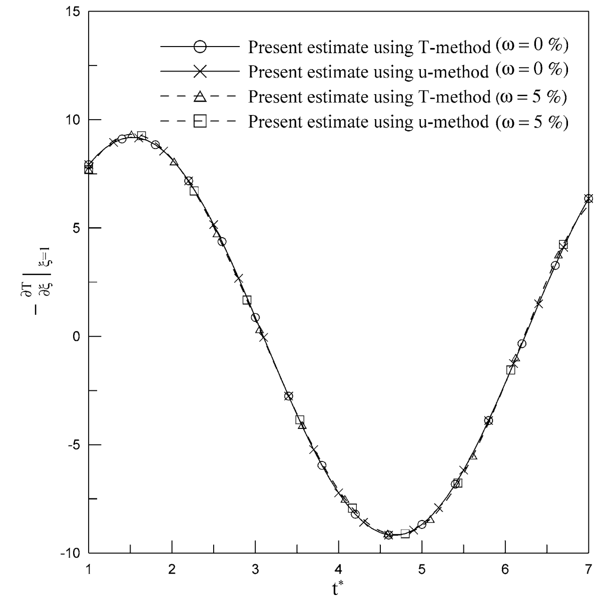

Fig. 4. Comparison of "$-(\partial T/\partial\xi)|_{\xi=1}$" for $F_1(t^*) = \sin(t^*)$, $\xi_m = 0.1$ and various ω values.

surface temperature $T(L,t)$ or $F_1(t)$ is also shown in Fig. 2. It can be observed from these two figures that the effect of the measurement location on the estimates of Grysa et al. [7] is not negligible. Their estimates [7] for $x_m = 0.9L$ are obviously smaller than those for $x_m = 0.7L$. This implies that the closer to the surface of the unknown boundary condition the measurement location, the more accurate the estimates of Grysa et al. [7]. It can also be found from Fig. 2 that the estimates of Grysa et al. [7] using the T-method are more accurate than those using the u-method. However, the present estimates using the T- and u- methods similarly are all in good agreement with the exact solution $T_{exa}(L,t)$. The cubic spline interpolation can be selected to fit the predicted values at $t = 0$, 1 and 2 s so that a single smooth curve can be obtained on the time interval 0 s $\leqslant t \leqslant$ 1 s.

In order to evidence the efficiency of the present inverse scheme further, the case with the unknown surface temperature $T(\xi = 1, t^*) = \sin(t^*)$ and the measurement error is also illustrated. The comparison of $T(\xi = 1, t^*)$ between the numerical results obtained from the direct problem and the present estimates using the T- and u-methods for $n = 11$, $\Delta t_e^* = 0.5$, $\xi_m = 0.1$, $M = 6$ and various ω values is listed in Fig. 3. Once the unknown surface temperature is determined, its corresponding unknown surface heat flux $q(\xi = 1, t^*)$ can also be computed. Thus the effects of the measurement errors on the estimation of the unknown temperature gradient "$-(\partial T/\partial\xi)|_{\xi=1}$" for $\omega = 0\%$ and $\omega = 5\%$ are shown in Fig. 4. The results show that the deviations of $T(\xi = 1, t^*)$ and "$-(\partial T/\partial\xi)|_{\xi=1}$" between the present estimates using the T- and u-methods and the numerical results obtained from the direct problem are small even for the interior measurements with the measurement error $\omega = 5\%$.

4.2. Example 2: Unknown surface heat flux $q(\xi = 1, t^*)$

The second inverse problem with $q(\xi = 1, t^*)L/k = -\frac{\partial T}{\partial \xi}|_{\xi=1} = \sin(t^*)$ is illustrated. In order to predict the unknown surface temperature $T(\xi = 1, t^*)$, the fourth degree polynomial guess function ($N = 3$) is selected to approximate $T(\xi = 1, t^*)$ or $F_1(t^*)$ on each sub-time domain for this inverse calculation. The unknown coefficients $C_j (j = 1, 2, 3)$ used to begin the iteration are taken as unity. The comparison of $T(\xi = 1, t^*)$ between the direct solution and the present estimates using the T- and u-methods is listed in Fig. 5 for $t_0^* = \alpha t_0/L^2 = 1$, $n = 11$, $\Delta t_e^* = 0.5$, $\xi_m = 0.1$, $M = 6$ and various ω values. Similarly, the unknown surface heat flux can also be determined using the obtained estimates of the unknown surface temperature. The comparison of the unknown surface temperature gradient "$-(\partial T/\partial \xi)|_{\xi=1}$" between the direct solution and the present estimates for $\omega = 0\%$ and $\omega = 5\%$ is shown in Fig. 6. It can be observed from Figs. 5 and 6 that the deviations of $T(\xi = 1, t^*)$ and "$-(\partial T/\partial \xi)|_{\xi=1}$" between the direct solution and the present estimates are small even for the interior measurements with the measurement error $\omega = 5\%$.

4.3. Example 3: Unknown surface temperature $T(\xi = 1, t^*) = t^* + \sin(t^*) + \cos(t^*)$

In this example, the surface temperature $T(\xi = 1, t^*)$ is assumed to be unknown, and its functional form is assumed as $T(\xi = 1, t^*) = F_1(t^*) = t^* + \sin(t^*) + \cos(t^*)$. The second degree polynomial guess function ($N = 3$) is selected to approximate the unknown surface temperature $T(\xi = 1, t^*)$ on each sub-time domain. The initial guesses of C_1, C_2 and C_3 are $C_1 = C_2 = C_3 = 0.1$. In order to investigate the effects of the dimensionless measurement time step Δt_e^* and the space size $\ell = 1/(n-1)$ on $T(\xi = 1, t^*)$, three different data ($\Delta t_e^* = 1$, $M = 6$, $n = 31$, $\ell = 1/30$) ($\Delta t_e^* = 0.1$, $M = 60$, $n = 11$, $\ell = 1/10$) and ($\Delta t_e^* = 0.05$, $M = 120$, $n = 11$, $\ell = 1/10$) are used to predict $T(\xi = 1, t^*)$. Table 2 shows the comparison of $T(\xi = 1, t^*)$ between the present estimates using the T- and u-methods and the direct solution for $\xi_m = 0.1, \omega = 0$ and various ℓ and Δt_e^* values. It can be observed from Table 2 that the differences of the present estimates obtained from ($\Delta t_e^* = 1$, $M = 6$, $n = 31$, $\ell = 1/30$) ($\Delta t_e^* = 0.1$, $M = 60$, $n = 11$, $\ell = 1/10$) and ($\Delta t_e^* = 0.05$, $M = 120$, $n = 11$, $\ell = 1/10$) are small. This implies that the present estimates are not very sensitive to Δt_e^* and ℓ. However, the smaller values of Δt_e^* and ℓ can need to be chosen provided that a more accurate estimation on the unknown surface temperature and

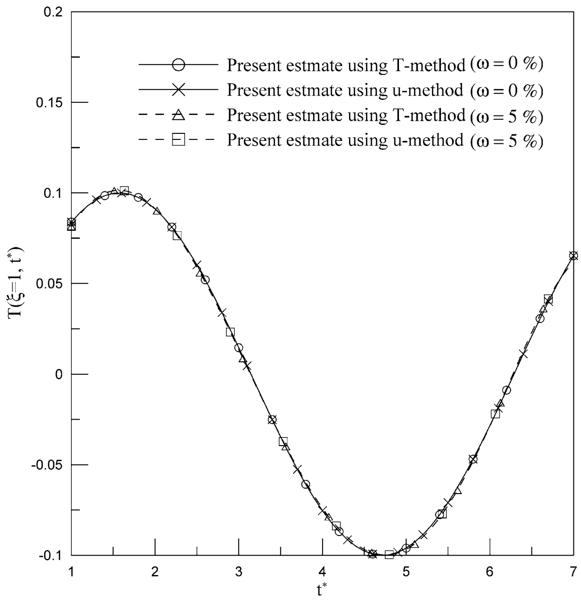

Fig. 5. Comparison of $T(\xi = 1, t^*)$ for "$-(\partial T/\partial \xi)|_{\xi=1} = \sin(t^*)$", $\xi_m = 0.1$ and various ω values.

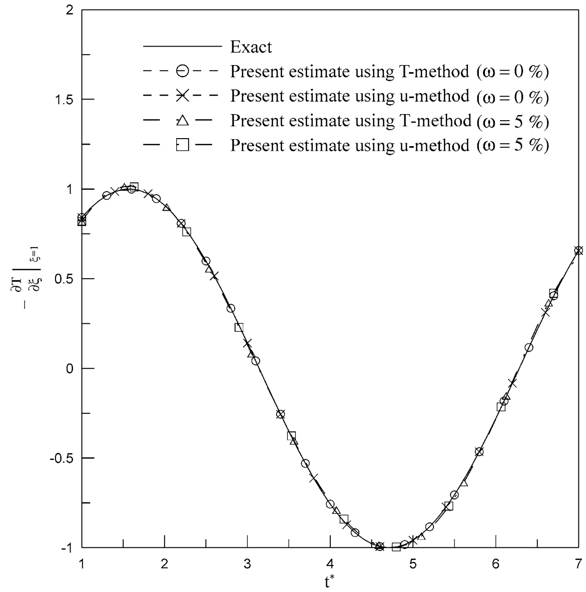

Fig. 6. Comparison of "$-(\partial T/\partial \xi)|_{\xi=1}$" for "$-(\partial T/\partial \xi)|_{\xi=1} = \sin(t^*)$", $\xi_m = 0.1$ and various ω values.

Table 2
Present estimates of $T(\xi = 1, t^*)$ using the T- and u-methods for $\xi_m = 0.1$, $\omega = 0$ and various ℓ and Δt_e^* values

t^*	T-method			u-method			Direct solution
	$\Delta t_e^* = 1$, $\ell = 1/30$	$\Delta t_e^* = 0.1$, $\ell = 1/10$	$\Delta t_e^* = 0.05$, $\ell = 1/10$	$\Delta t_e^* = 1$, $\ell = 1/30$	$\Delta t_e^* = 0.1$, $\ell = 1/10$	$\Delta t_e^* = 0.05$, $\ell = 1/10$	
1	2.3821	2.3821	2.3820	2.3822	2.3822	2.3821	2.3818
3	2.1511	2.1510	2.1511	2.1512	2.1512	2.1513	2.1511
5	4.3248	4.3248	4.3247	4.3246	4.3245	4.3246	4.3247
7	8.4108	8.4107	8.4108	8.4107	8.4105	8.4108	8.4109
9	8.5011	8.5013	8.5011	8.5012	8.5013	8.5011	8.5010
11	10.0042	10.0039	10.0043	10.0039	10.0036	10.0043	10.0044
13	14.3276	14.3275	14.3276	14.3275	14.3277	14.3275	14.3276

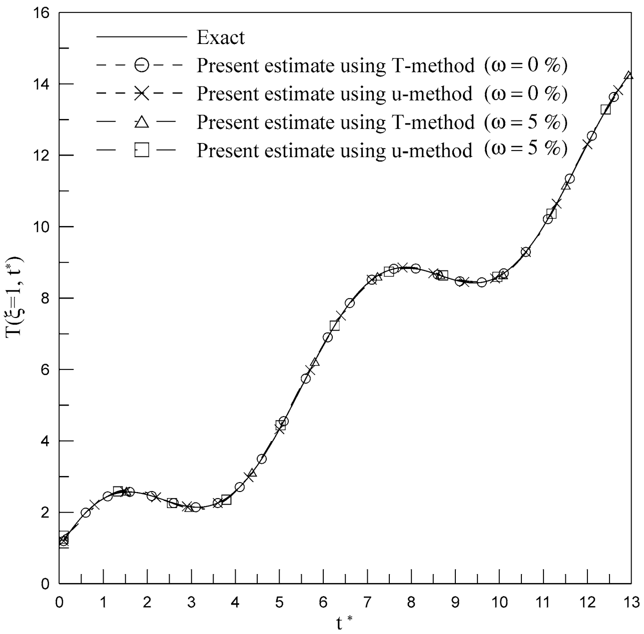

Fig. 7. Comparison of $T(\xi = 1, t^*)$ for $F_1(t^*) = t^* + \sin(t^*) + \cos(t^*)$, $\xi_m = 0.1$ and various ω values.

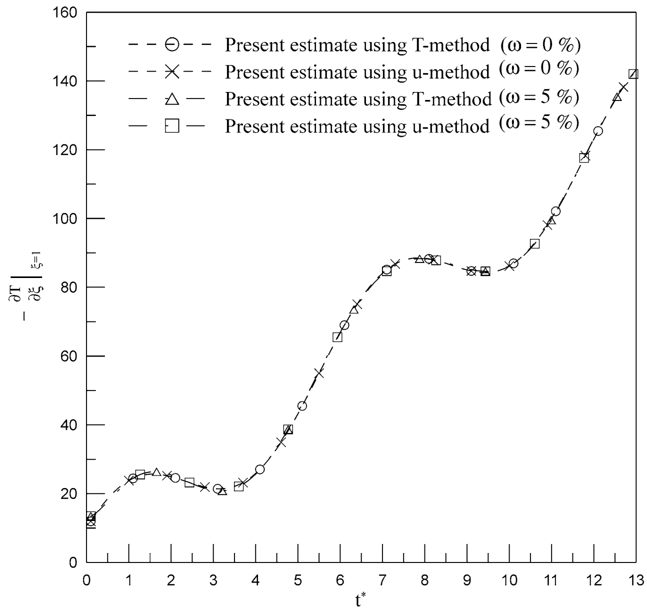

Fig. 8. Comparison of "$-(\partial T/\partial\xi)|_{\xi=1}$" for $F_1(t^*) = t^* + \sin(t^*) + \cos(t^*)$, $\xi_m = 0.1$ and various ω values.

the unknown surface heat flux is required. Relatively, a more computational time can be required for these cases. The comparisons of $T(\xi = 1, t^*)$ and "$-(\partial T/\partial\xi)|_{\xi=1}$" between the present estimates using the T- and u-methods and the direct solution are, respectively, shown in Figs. 7 and 8 for $t_0 = 0s$, $\xi_m = 0.1$, $\Delta t_e^* = 0.1$, $n = 11$ and various ω values. It can be found from these two figures that the deviations of $T(\xi = 1, t^*)$ and "$-(\partial T/\partial\xi)|_{\xi=1}$" between the present estimates and the numerical results obtained from the direct problem are small even for the interior measurements with the measurement error $\omega = 5\%$ over the whole time domain $0 \leqslant t^* \leqslant 12$. This implies that the present estimates perform stable behavior even for the interior measurements with the measurement error. In addition, the initial guesses of $C_1 = C_2 = C_3 = 1$ and $C_1 = C_2 = C_3 = 10$ are also used to estimate $T(\xi = 1, t^*)$ and "$-(\partial T/\partial\xi)|_{\xi=1}$". These predicted results for $C_1 = C_2 = C_3 = 1$ and $C_1 = C_2 = C_3 = 10$ are not shown in this manuscript because they are in good agreement with the estimates shown in Figs. 7 and 8. These results mean that the effect of the initial guesses on the present estimates is not significant for the present inverse scheme.

5. Conclusion

The present study proposes a numerical simulation involving the Laplace transform technique and the finite-difference method in conjunction with a sequential-in-time concept and the least-squares method to estimate the histories of the unknown surface temperature and the unknown surface heat flux for various kinds of the boundary conditions using the T- and u-methods. *The number of iterations is four times for the u-method and three times for the T-method. However, the computational time of the present inverse scheme for obtaining the available estimates of the unknown surface temperature and unknown surface heat flux of the present three examples is about* 5 s *on PC PIII-500*. Owing to the application of the Laplace transform scheme, the unknown surface temperature and the unknown surface heat flux can be estimated simultaneously from a specific time. It is found from various illustrated examples that the present inverse scheme can give a good estimation on the unknown surface temperature and the unknown surface heat flux even for the interior measurements with the measurement error. The advantages of the present inverse scheme are not very sensitive to the initial guesses of the unknown coefficient, the measurement location and the interior measurements. *In order to obtain a more accurate estimation on the unknown surface temperature and the unknown surface heat flux for the present inverse method, the smaller value of Δt_e^* and the space size ℓ can be chosen*.

References

[1] M.N. Özisik, Heat Conduction, second ed., Wiley, New York, 1993, Chapter 14.
[2] E. Hensel, Inverse Theory and Applications for Engineers, Prentice-Hall, Englewood Cliffs, NJ, 1991.
[3] K. Kurpisz, A.J. Nowak, Inverse Thermal Problems, Computational Mechanics Publications, Southampton, UK, 1995.
[4] H.Y. Li, M.N. Özisik, Identification of the temperature profile in an absorbing, emitting, and isotropically scattering medium by inverse analysis, J. Heat Transfer 114 (1992) 1060–1063.
[5] J.V. Beck, B. Blackwell, A. Haji-Sheikh, Comparison of some inverse heat conduction methods using experimental data, Internat. J. Heat Mass Transfer 39 (1996) 3649–3657.

[6] G. Cloud, Optical Methods of Engineering Analysis, Cambridge University Press, Cambridge, 1998.

[7] K. Grysa, M.L. Cialkowsky, H. Kaminski, An inverse temperature field problem of the theory of thermal stresses, Nuclear Engrg. Design 64 (1981) 169–184.

[8] G. Blanc, M. Raynaud, Solution of the inverse heat conduction problem from thermal strain measurements, ASME J. Heat Transfer 118 (1996) 842–849.

[9] E.M. Sparrow, A. Haji-Sheikh, T.S. Lundgren, The inverse problem in transient heat conduction, J. Appl. Mech. 86e (1964) 369–375.

[10] K.W. Woo, L.C. Chow, Inverse heat conduction by direct inverse Laplace transform, Numer. Heat Transfer 4 (1981) 499–504.

[11] M. Monde, Analytical method in inverse heat transfer problem using Laplace transform technique, Internat. J. Heat Mass Transfer 43 (2000) 3965–3975.

[12] H.T. Chen, S.M. Chang, Application of the hybrid method to inverse heat conduction problems, Internat. J. Heat Mass Transfer 33 (1990) 621–628.

[13] H.T. Chen, S.Y. Lin, L.C. Fang, Estimation of surface temperature in two-dimensional inverse heat conduction problems, Internat. J. Heat Mass Transfer 44 (2001) 1455–1463.

[14] H.T. Chen, S.Y. Lin, L.C. Fang, Estimation of two-sided boundary conditions for two-dimensional inverse heat conduction problems, Internat. J. Heat Mass Transfer 45 (2002) 15–23.

[15] H.T. Chen, S.Y. Peng, P.C. Yang, L.C. Fang, Numerical method for hyperbolic inverse heat conduction problems, Internat. Comm. Heat Mass Transfer 28 (2001) 847–856.

[16] H.T. Chen, X.Y. Wu, Application of the hybrid method to the estimation of surface conditions from experimental data, in: Trends in Heat, Mass and Momentum Transfer, India, 2003, submitted for publication.

[17] H.Y. Li, Theoretical and experimental studies of the inverse heat conduction problems, Report of National Council Science, NSC 87-2212-E-211-007, 1998.

[18] R.B. Hetnarski, Basic equations of the theory of thermal stresses, in: R.B. Hetnarski (Ed.), Thermal Stress I, North-Holland, Amsterdam, 1986, pp. 1–21.

[19] J.P. Holman, W.J. Gajda Jr, Experimental Methods for Engineers, fifth ed., McGraw-Hill, New York, 1989, pp. 37–83.

[20] W.M. Dubner, J. Abate, Numerical inversion of Laplace transforms by relating them to the finite Fourier cosine transform, J. Assoc. Comput. Math. 15 (1968) 115–123.

[21] F. Durbin, Numerical inversion of Laplace transforms: Efficient improvement to Dubner and Abate's method, Comput. J. 17 (1973) 371–376.

[22] G. Honig, U. Hirdes, A method for the numerical inversion of Laplace transforms, J. Comput. Appl. Math. 10 (1984) 113–132.